Praseodymium Yttrium Fluoride Lithium (Pr:YLF) Green-Lasers and its Excited State Absorption(ESA) Spectra

A Thesis

Presented to the Faculty of the Graduate School

of Cornell University

In Partial Fulfillment of the Requirements for the Degree of

Master of Science

by

Jayakrishnan Appanam Karakkad

August 2014

ABSTRACT

Solid state visible lasers have various applications in the field of color display, holographic techniques, data storage and medical treatment. So far green laser output has been obtained using methods of frequency conversion, thus increasing the cost of building the laser as well due to the low efficiency of such techniques. There are very few materials which produce visible laser radiation directly. Trivalent Praseodymium (Pr^{3+}) is one such example. It is quite interesting because of its unique energy scheme which offers multiple transitions in the visible spectrum. We are mainly interested in the energy transition from $^3P_0$ to $^3H_5$ which produces light in the green visible spectrum (523 nm).

Green lasers are particularly useful and important in certain types of underwater communications. Sea water has low absorbance and offers relatively low scattering for green light, thus making green light one of the most effective sources for underwater communications. Excited State Absorption (ESA) is a phenomenon where absorption occurs from an occupied excited state level of the specie. This can lead to additional loss, which causes complications for lasing in the form of increased threshold power, reduced power slope efficiency, and change in lasing wavelength due to offset in the highest emission cross-section. This thesis examines the spectroscopic profile of Praseodymium-doped Yttrium Lithium Fluoride (Pr:YLF) including the ground state absorption, fluorescence, and ESA in great detail. We explore the experimental setups used, detection scheme and finally reveal the results obtained.

BIOGRAPHICAL SKETCH

Jayakrishnan Appanam Karakkad was born Wednesday the 27th of March, 1991 in Kerala, India. The second son of Geetha and Subramanian, he spent his early days as a mischievous young boy busy getting in trouble. After completing his various parts of schooling in Kerala, Lucknow, and Bangalore he completed his Higher Secondary education in the prestigious Kendriya Vidyalaya Malleswaram with full distincition. He appeared in the Joint Entrance Examination in 2008 and was admitted into the Indian Institute of Technology Guwahati (IIT G) where he pursued his bachelors in Engineering Physics. The institute gave him various experiences including a deep passion for basketball, classical music and game designing. Academically the institute developed a keen mind for optics and photonics that has led him to this point in his life. His studies led him to take up internship in a startup fiber optics company in 2010 and work as an intern in Indian Institute of Science Bangalore at the lab of Prof.Asokan. He finally finished his Bachelors thesis under the guidance of Prof.Khijwania (IIT G). These experiences hardened his resolve to pursue higher studies in the field of optics.

In the fall 2012 he enrolled at Cornell University in the M.S, Applied Engineering Physics program. He worked under the guidance of Prof. Clifford Pollock, studying the spectroscopic profile of Pr:YLF and searching for the existence of ESA in the visible spectrum.

Dedicated to Ma and Achan.

ACKNOWLEDGMENTS

I would like to first thank my advisor, Prof. Clifford R. Pollock, who has been an excellent guide over the past year. I have found him to be an excellent teacher and researcher who has helped me through various obstacles and problems. At various points during my thesis when the going became tough, his valuable inputs helped me continue forward in the right direction.

I would also like to thank Prof. Frank W. Wise for consenting to be my second committee member and for providing his valuable advice and inputs. A significant amount of my interaction with him has been outside the scope of my M.S thesis, in the form of lectures and as his teaching assistant. I have found him to be very understanding and approachable.

Next I would like to thank the members of the Pollock Group for their valuable insights and guidance. Victor for his help and advice when I was still new and green in the lab. Ang for his help and advice in building the experimental setup. Kyung for her expertise and for sharing the workload involved in the experiments.

I would also like to thank my friends here at Cornell who have supported me throughout of my stay in Ithaca. Avik, Hapshi, Ashish, Bhatia, Chotu, Kakat and rest of the gang, you guys have made my stay in Cornell all the more enjoyable and fun.

Lastly I would like to thank my parents and my brother for always supporting me through various difficult times in my life.

TABLE OF CONTENTS

LIST OF FIGURES

LIST OF TABLES

LIST OF ABBREVIATIONS

nm : Nanometer

GaN : Gallium Nitride

ESA : Excited State Absorption

UV : Ultraviolet

IR : Infrared

GSA : Ground State Absorption

Chapter 1
Introduction

In recent years, solid-state visible lasers have become a readily available commodity, we use them in our day to day life for various purposes. They are being studied in depth due to their applications in the fields of color display, communication, and medicine. Many of these solid-state visible laser lines have been obtained via methods of frequency conversion such as frequency doubling, sum, and difference frequency generation [10]. While these methods are still very popular, the increase in cost due to complexity and loss of power due to low conversion efficiency have always stimulated researchers to explore alternate sources.

Let us take the case of how a normal green laser pointer works. First light is generated at 808 nm using an electrically driven semiconductor diode laser, which is then used to pump a Neodymium-doped Yttrium Vanadium Oxide crystal, which lases at 1064 nm. This output is then frequency doubled via a non-linear crystal (KTP in this case) to obtain the desired green light at 532 nm. This increased complexity increases the cost of production, while the efficiency is generally reduced due to losses incurred during the non-linear frequency conversion.

Trivalent Praseodymium (Pr^{3+}) is very interesting due the fact that it has emission lines spread out throughout the visible spectrum. It has a unique energy level setup which offers emissions ranging from green (523 nm, $^3P_0 \rightarrow {}^3H_5$), orange (607 nm, $^3P_0 \rightarrow {}^3H_6$), red (640 nm, $^3P_0 \rightarrow {}^3F_2$), and dark red (720 nm, $^3P_0 \rightarrow {}^3F_3 + {}^3F_4$). The Pr:YLF sample thus offers a promising venue for producing visible blue, green and red lasers.

Fig.1 below shows the Pr^{3+} energy bands. The first reported study of absorption and emission cross-section of Pr:YLF was in 1962[1]. The lack of a suitable blue pump source was one of the main issues faced in realizing cost-effective Pr^{3+} lasers. A large variety of pump sources have been used to produces lasers operating from 479 nm to 907.4 nm[2]. After the invention of the GaN blue diode laser (445 nm), production of cheaper and smaller Pr:YLF became possible.

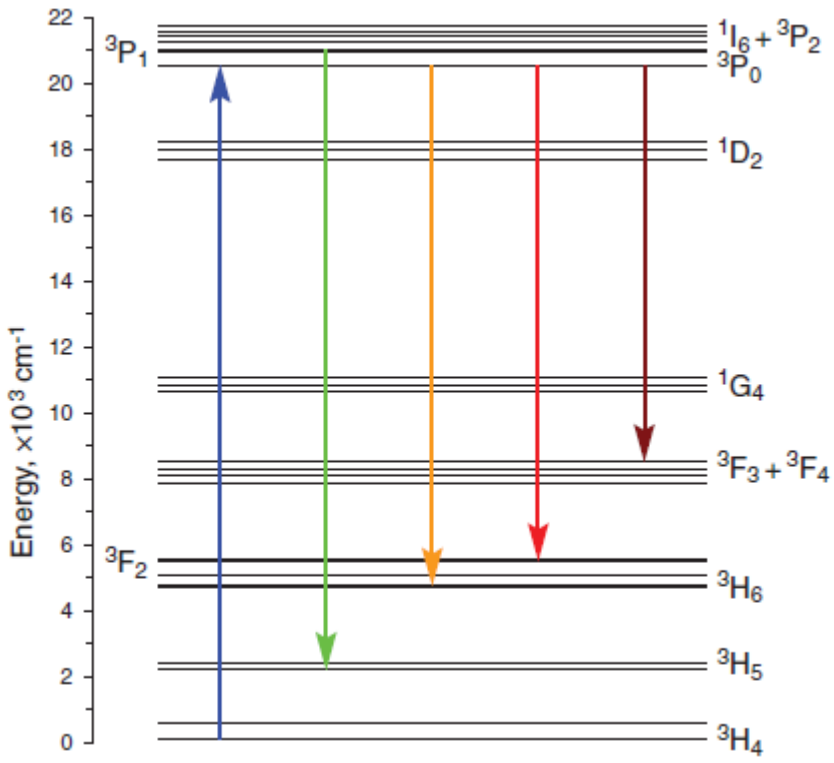

Fig.1: Energy levels of Pr:YLF.

In this thesis we have used a GaN blue diode laser with a base power of 1.5W as the pump source.

An important part of this thesis involves looking for the phenomenon called as Excited State Absorption (ESA). The presence of ESA at the pump wavelength(445 nm) can increase the threshold power required for creating the green lasers, similarly the presence of ESA at the emission wavelength(523 nm) can lead to several undesirable effects.

In chapter 2 we shall look at the theory behind the different spectroscopic setups and techniques we use to obtain Ground State Absorption (GSA), Fluorescence, and ESA.

In Chapter 3 we mainly discuss more about the GaN diode laser and the steps taken to collimate its output beam. We shall also look into different parameters such as

expected lifetime of the excited state, saturation intensity required. The results of a small Q-switching simulation is also discussed in this chapter.

Chapter 4 will contain the results obtained from the GSA, Fluorescence and ESA measurements taken. We will also discuss the conclusions drawn from the experiments.

Chapter 2

Theoretical Review of the Spectroscopy of Pr^{3+}

2.1 Ground State Absorption

The absorption spectrum of stable atoms and molecules is most easily studied using a scanning spectrophotometer. This setup basically consists of a light source which can emit a broad spectrum of light from the UV to the Infrared, a monochromater to narrow down the wavelength range being studied, the sample holder and finally the detection setup.

The sample is irradiated using a continuous wave source and the fraction of light absorbed is determined either by transmission or reflectance measurements. Light absorption sends the atom or molecule to an excited state and thus the information obtained via the measurements will pertain to the absorption spectrum of the sample, the energy difference between ground state and the excited state.

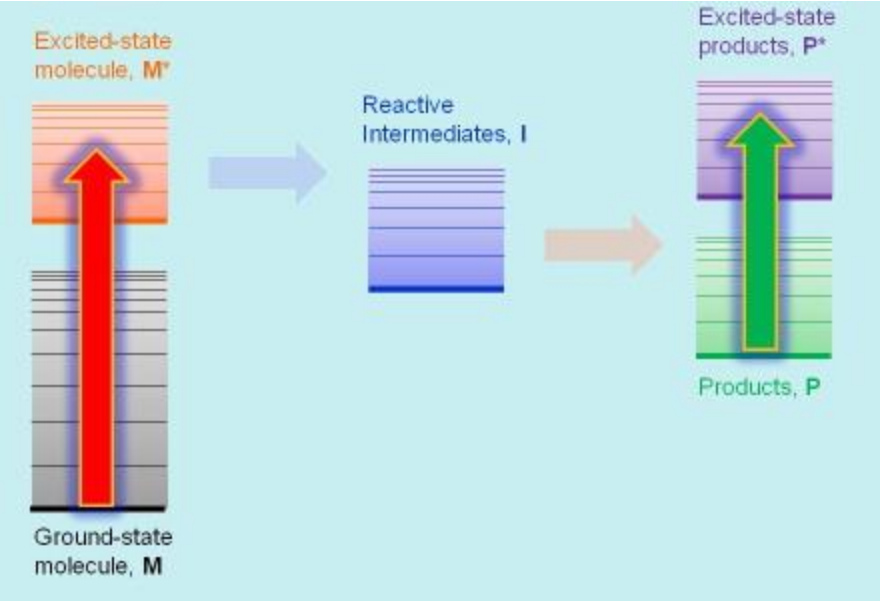

Fig.2: Energy transitions in GSA.

The transmittance of a transparent sample is the amount of light it lets through it when it is irradiated. The transmittance can be measured by comparing the intensity of the

beam before entering the crystal and intensity of light exiting the crystal. A plot of transmittance vs wavelength gives the transmission spectrum. The ground state absorption can be easily obtained from transmission spectrum by taking the negative logarithm of transmittance.

$$\text{Absorbance (A)} = -\log(\text{Transmittance}) \qquad (2.1)$$

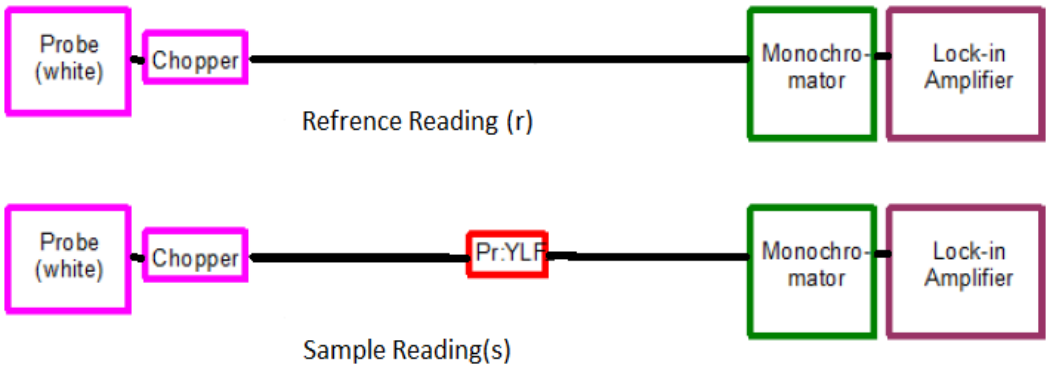

Fig.3: A figure showing the experimental setup used for obtaining the GSA

2.2 Transient Absorption

When the species being studied is meta-stable (transient) we get something called transient absorption. The lifetime of the excited interstate may range from a few femtoseconds (in cases of primary excited states) to kilo seconds.

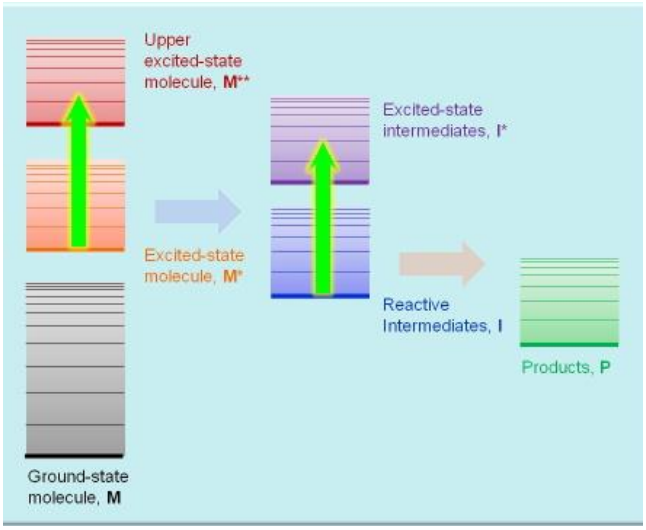

Fig.4: Energy transitions in Transient absorption.

The measurement involves the use of a pulsed laser for exciting the sample to required concentration and a second source, continuous wave or pulsed for probing the absorption. Transient absorption spectroscopy techniques involves the use of a probe beam which interrogates the sample before and after being exposed to a secondary source (CW or pulsed), while constantly monitoring the change in absorbance.
The pump laser needs to fulfill certain criteria for proper measurement to occur, namely:

1) The pump laser must work at a wavelength where GSA occurs.
2) The laser pulse width must be shorter than the time constant of the change being measured.

The probe beam is a broad band source covering UV to IR wavelengths. The parameter which is measured is change in absorbance (ΔA). This is obtained by noting the change in intensity of transmitted probe light before (I_0) and after (I) excitation by the pump laser. The change in absorbance is obtained using the following equation.

$$\Delta A = -\log(\frac{I}{I_0}) \qquad (2.2)$$

2.3 Emission Spectroscopy

In emission spectroscopy a sample is irradiated using a suitable light source, the luminescence emerging from the sample is then measured using a suitable detector. The luminescence is caused by the decay of the excited states to the ground state. When the excited state has the same spin state as the ground state we call the decay as fluorescence. When the transition is forbidden or in other words the spins are different we get phosphorescence. Fluorescence process usually lasts anywhere from a few nanoseconds to hundreds of microseconds, while phosphorescence may last anywhere between milliseconds to hours. It is also seen that phosphorescence occurs at longer wavelengths compared to fluorescence. In this thesis we are particularly only interested in the fluorescence spectra of Pr:YLF. Emission spectra is obtained by exciting the sample at a fixed wavelength and then scanning the monochrometer over the wavelength range needed.

2.4 Excited State Absorption

In a solid state crystal, it can occur that the upper state population not only leads to stimulated emission but also absorption process, which can excite the laser ions to a higher excited state. This process factors in as additional loss, which can thus raise the threshold pump power needed and also reduce the slope efficiency. ESA can sometimes cause a laser to operate at a wavelength that is offset from that of its highest emission cross-section.

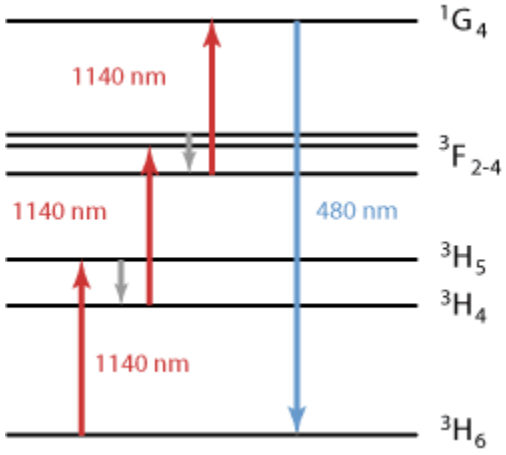

Fig.5: Excitation of higher states of thulium via ESA.

ESA is commonly seen in broad band gain mediums like transition metal doped crystals and rarely in narrow band gain mediums like rare earth doped crystals. ESA is more likely to be common in laser ions having multiple electronic levels such as erbium and thulium. The above figure (Fig. 5) shows an example of ESA seen in thulium (3+) ions.

ESA is also common in saturable absorbers. Saturable absorber is an optical component with certain optical loss, which is reduced at high intensities. The ground state absorption in such cases can be fully bleached, however the excited state absorption remains since it recovers much more quickly, even at high optical intensities. Effectively ESA causes roughly one-thirds of the saturable losses in the form of non-saturable loss[7].

2.4.1 ESA in up-conversion lasers

It should be mentioned that although ESA is normally a detrimental force, in certain cases it can be used to one's advantage. It is highly useful in upconversion pumping. When a medium emits fluorescence upon absorption of light, the wavelength of fluorescence is usually longer than the wavelength of the exciting light, which in turn means a reduced photon energy. However with the help of ESA one can sometimes ensure upconversion fluorescence, where the wavelength of the emitted light is shorter. Fig.5 shows an example of upconversion, with the blue line representing the short wavelength fluorescence.

2.4.2 Measuring ESA cross-section

In certain cases, factoring the impact of ESA into the laser operation may be simple. For example if ESA leads to ions going to higher states which have very short lifetimes then ESA can be factored into the calculation as another absorption term. Fortunately Pr:YLF falls into this category.

We shall first look at an experimental setup which was used to measure ESA in erbium-doped fibers [3]. The setup is shown below in Figure 6.

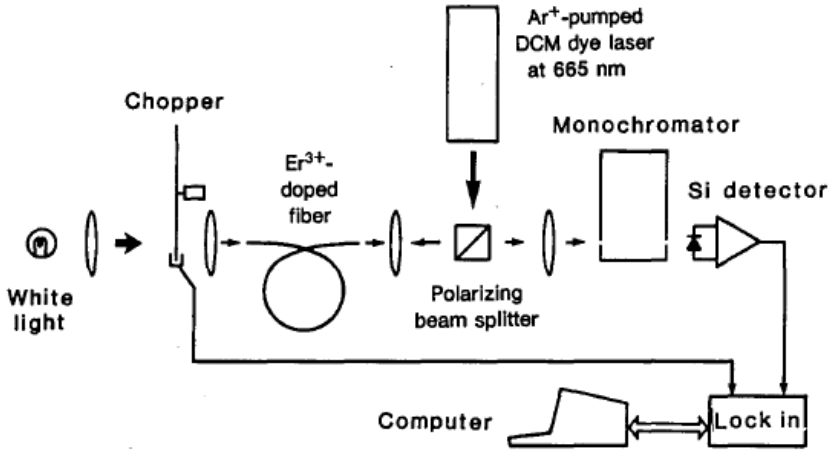

Fig.6: Experimental setup to measure ESA in erbium doped fibers

The setup consists a broad band source which acts as a probe. A second light source (usually CW) is used to excite the sample. The probe beam is modulated using a chopper. The lock in amplifier is tuned to the chopping frequency of the probe beam.

In this kind of setup first the ground state absorption is measured with the pump switched off (in this case the argon pump). Next the pump is switched on and we measure the new absorption. The change in absorption gives us the ESA measurement. A positive change in absorbance indicates the presence of ESA.

The reasoning behind this is that the presence of ESA will increase the absorption at that particular wavelength and thus the change in absorption will be positive. This is also the reason why it is quite difficult to detect weak ESA since there is no way to differentiate it from random noise. The only way around this problem is to fine tune different parts of the setup to minimize the noise level.

One can also use a dual chopping scheme to measure ESA with a greater accuracy [4]. The following equations describe the intensity of the beam through the crystal when the pump is on and off [4].

$$I_{unpumped} = I_0 \exp(-\sigma_{GSA} n L) \quad (2.3)$$

$$I_{pumped} = I_0 \exp[-\sigma_{GSA}(n - n_e)L + \sum_i \left(\frac{n_i}{n_e}\right)(\sigma_{em,i} - \sigma_{ESA,i}) n_e L] \quad (2.4)$$

Where I_0 is the probe intensity, n_i is the population density of excited state i, σ_i is the cross-section of transition i, n_e and n are the excited state population density and total ground state population respectively, and L is the total length of the crystal.

Combining equation (2.3) with (2.4) we get,

$$\ln[1 + \left(\frac{I_{pumped} - I_{unpumped}}{I_{unpumped}}\right)] = n_e L(-\sigma_{GSA} - \sum_i \left(\frac{n_i}{n_e}\right)(\sigma_{em,i} - \sigma_{ESA,i}))] \quad (2.5)$$

Since the difference between I_{pumped} and $I_{unpumped}$ is quite small we can make the approximation

$$\ln\left[1 + \left(\frac{I_{pumped} - I_{unpumped}}{I_{unpumped}}\right)\right] = \frac{\Delta I}{I_{unpumped}} \quad (2.6)$$

For the same reason we can also say replace the $I_{unpumped}$ term with the simple probe beam intensity I.

Another way to detect ESA is to modulate the pump beam instead of the probe beam[5]. This method can only be used when the relaxation time (lifetime) of the excited state is very small compared to the modulation frequency of the pump beam. The chopped beam, along with fast relaxation time creates a time dependent

populations in the excited state and the ground state. The populations in the excited state and the ground state will be in-phase and out-of-phase with the pump laser, respectively.

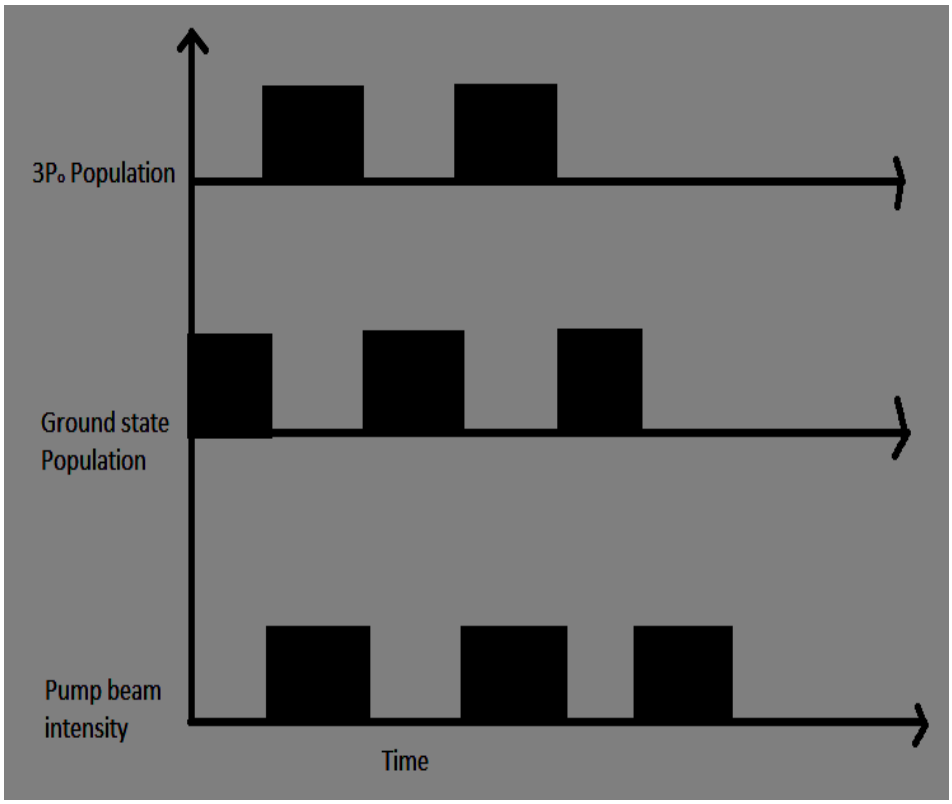

Fig.7: A diagram depicting the excited state and ground state population (in Pr:YLF) in respect to pump beam.

Fig. 7 shows an example of pumping the 3H4 – 3P0 level of Pr 3+. The excited state absorption signals arising from $3P_0$ therefore appear out-of-phase with the pump, while absorption signals originating from the ground state,$3H_4$, appear in phase with the pump. The modulation signals of the absorption spectrum are monitored using a lock-in amplifier at the chopping frequency of the pump laser.

Chapter 3

GaN DIODE LASER AND Q-SWITCHING

3.1 GaN Blue Diode Laser

Researchers have sought to deposit GaN on sapphire to build blue lasers since 1960. The first GaN blue laser however was made by Shuji Nakamura in 1996[6].

We obtained a 1.5 W GaN blue diode laser from LDX optronics. The laser is highly multimode and has high divergence of about 12^o in the X, and 40^oin Y axis. We were also interested in the shape of the laser output since we wanted an intense uniform square shape for maximum overlap with the probe beam. The output of the laser beam diverges asymmetrically, thus making collimating the laser beam an immense challenge. Using spherical optics would result in collimating only one direction, leaving us with a diverging beam in the other direction. Cylindrical lenses were used to restrict the divergence along the X and Y axis to change the shape of the beam. The Fig.8 below shows the use of cylindrical lenses to change an elliptical beam to circular.

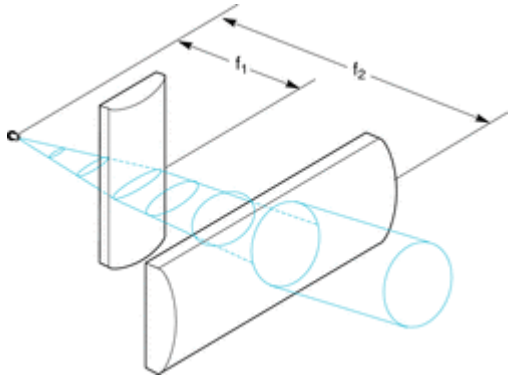

Fig.8: An elliptical beam modified into a circular beam using cylindrical optics

The following points helped us in selecting and placing the cylindrical lenses:

1) The ratio of the focal lengths of the cylindrical lenses must approximately equal the ratio of divergences.

$$\frac{\theta_1}{\theta_2} = \frac{f_1}{f_2} \qquad (3.1)$$

2) Since we are approximating the laser source as a point source the lenses should be placed at a distance approximately equal to their focal lengths to create a collimated output.
3) The principle planes of the lenses should be placed in such a way that the distance between them is equal to the difference in their focal lengths. Just like in case of spherical lenses, the convex side should face the collimated rays so as to avoid aberrations.
4) The laser beam diverges at a fast pace and thus we need to make sure that the beam width of the laser beam did not exceed the lens clear aperture. The maximum permissible beam width at each lens b_2 and b_2 is given by,

$$b_i = 2f_i \tan(\frac{\theta_i}{2}) \qquad (3.2)$$

The reason why we are taking such extreme care in collimating the laser beam is because we want to collect maximum power to ensure a sizeable population excitation. This would thus enable us to differentiate ESA readings from the noise. Three cylindrical lenses with focal lengths 2cm, 4.7cm and 15cm were used to collimate and shape the laser output. The cylindrical lens with focal length of 2cm was placed on top of the laser to restrict the divergence along the Y axis (40^o) or else the beam spreads out and grows larger than the lens clear aperture. Next the cylindrical lens with focal length of 4.7 cm was placed at a distance of 5 cm from the laser to restrict divergence along X axis. Finally the last cylindrical lens was placed at a distance of 14.5 cm from the laser to restrict divergence along Y axis. The resulting beam was uniformly square shaped with a constant 7x7 cm^2 cross-section. The beam shape got distorted after travelling a distance of 160cm, but this was fine since it was within the standards we required. In collimating the beam only the fundamental and the next mode was collected since it carried the majority of laser output power. The exclusion of the higher order modes and losses introduced at lens and mirror surfaces contributed to a total power loss of about 33%. This meant that the 1.5W laser beam output was reduced to 1W. Our aim was to focus this effective 1W power into the crystal in the shape of a tight square with sides of 100um.

3.2 Q-Switching

Q-switching is a technique by which a laser can produce a pulsed output beam. The pulse beam has high peak power. The high peak power which can range from MW to GW, is particularly useful in applications such as laser drilling, cutting or even pumping other laser systems. In a Q-switched laser, losses are intentionally introduced in such a way that population inversion can be built up to levels much greater than the threshold inversion for lasing. Once the population inversion has grown large enough the quality or "Q" of the cavity is switched back to normal or high. High rates of stimulated then cause the photon density to grow rapidly, depleting the population inversion density well below the normal limits. Q-switching is most effective in systems where the lifetime of the excited state is long as this allows the population inversion to grow without significant decay via spontaneous emission.

3.2.1 Q-switching analysis

Let us analyze the rate equations for a simple 2 level laser system. The rate equation can be written as,

$$\frac{dN_2}{dt} = R_2(t) - N^*(t)\sigma_{21}\frac{I(t)}{h^*\omega_l} - \frac{N_2(t)}{\tau_2} \qquad (3.3)$$

$$\frac{dN_1}{dt} = R_1(t) + N^*(t)\sigma_{21}\frac{I(t)}{h^*\omega_l} - \frac{N_1(t)}{\tau_1} + N_2(t)A_{21} \qquad (3.4)$$

Where R_i is the pump rate of level i, ω_l being the angular frequency, I(t) is the intensity of the oscillating laser mode, N^* is the population inversion density and N_i being the population density of level i. h^* is the reduced Planck's constant and A_{21} is the Einstein's A coefficient.

The rate equation for the density of photons can be simply written as,

$$\frac{dn_\emptyset}{dt} = f_c N^*(t)\sigma_{21}\frac{I(t)}{h^*\omega_l} - \frac{n_\emptyset(t)}{\tau_c} \qquad (3.5)$$

Where $n_\emptyset$ is the photon density, f_c is the fraction of oscillating mode lying within the gain medium and τ_c is the cavity lifetime.

This can be further reduced since $I(t) = n_\emptyset(t)ch^*\omega_l$, giving us equation (3.6). N_{th} represents the threshold inversion density in equation (3.6).

$$\frac{dn_\emptyset}{dt} = \left(\frac{N^*}{N_{th}} - 1\right)\frac{n_\emptyset(t)}{\tau_c} \qquad (3.6)$$

The Q-switching analysis can be made simple by assuming that the pump pulse duration is much larger compared to the Q-switched pulse. We also ignore spontaneous transitions. Thus equations (3.3) and (3.4) reduces to:

$$\frac{dN_2}{dt} = -N^*(t)\sigma_{21}\frac{I(t)}{h^*\omega_l} \tag{3.7}$$

$$\frac{dN_1}{dt} = N^*(t)\sigma_{21}\frac{I(t)}{h^*\omega_l} \tag{3.8}$$

Let degeneracy of energy level i be represented by g_i then, the population inversion rate equation during the Q-switched pulse can be obtained by the below equation:

$$\frac{dN^*}{dt} = \frac{dN_2}{dt} - \frac{g_2}{g_1}\frac{dN_1}{dt} = -\beta N^*(t)\sigma_{21}\frac{I(t)}{h^*\omega_l} \tag{3.9}$$

Where $\beta = 1 + {}^{g_2}/_{g_1}$.

The equations above represents cases with severe bottlenecking, where the rate of spontaneous decay of the lower level is negligible. It is thus assumed that stimulated emission is the only cause for the population to build up in the lower level.

In ideal four level laser systems, usually the lower levels decays very quickly and thus we can take $N_1(t) \approx 0$, thus making $N^*(t) \approx N_2(t)$.

Threshold inversion density is given by the equation [7]: $N_{th} = \frac{1}{f_c\sigma_{21}c\tau_c}$ and since $I(t) = n_\emptyset(t)ch^*\omega_l$ we can reduce equation (3.9) to:

$$\frac{dN^*}{dt} = -\frac{\beta}{f_c}\frac{N^*}{N_{th}}\frac{n_\emptyset}{\tau_c} \tag{3.10}$$

Next we use the fact that the initial and final density of photons in the cavity are both zero thus,

$$\int_{-\infty}^{\infty} dn_\emptyset = 0 \tag{3.11}$$

Using this with equation (3.5) gives us,

$$\int_{-\infty}^{\infty}\frac{N^*}{N_{th}}\frac{n_\emptyset(t)}{\tau_c}dt = \int_{-\infty}^{\infty}\frac{n_\emptyset(t)}{\tau_c}dt \tag{3.12}$$

The rate at which photons coupled out of laser is equal to $n\frac{V_c}{\tau_c}$, where V_c represents the volume of oscillating mode within the cavity. Thus power output is,

$$P = h^*\omega_l n_\emptyset\frac{V_c}{\tau_c} \tag{3.13}$$

Integrating equation (3.13) with respect to time and applying equation (3.12) we get,

$$E = h^* \omega_l V_c \int_{-\infty}^{\infty} \frac{N^*}{N_{th}} \frac{n_\emptyset(t)}{\tau_c} dt \qquad (3.14)$$

Next using equation (3.10) we substitute for dt to get,

$$E = -h^* \omega_l V_c \frac{f_c}{\beta} \int_{N^*_{initial}}^{N^*{}_{final}} dN^* \qquad (3.15)$$

Where $N^*_{initial}$ and N^*_{final} are initial and final population inversion densities.

Let V be the volume of oscillating mode in the gain medium, then $V = f_c V_c$ thus equation (3.15) becomes:

$$E = h^* \omega_l \frac{V}{\beta} (N^*_{initial} - N^*{}_{final}) \qquad (3.16)$$

In Q-switching the final population inversion density becomes almost zero after the Q-switched pulse is formed.

Dividing equation (3.6) with equation (3.10) and integrating gives us,

$$\int_{-\infty}^{t} dn_\emptyset = \frac{f_c}{\beta} \int_{-\infty}^{t} (\frac{N^*}{N_{th}} - 1) dN^* \qquad (3.17)$$

$$n_\emptyset = \frac{f_c}{\beta} [N_{th} \ln(\frac{N^*(t)}{N^*_{initial}} + N^*_{initial} - N^*(t)] \qquad (3.18)$$

Let us define the ratio of initial population inversion to threshold inversion as r, the overpumping ratio.

$$r = \frac{N^*_{initial}}{N_{th}} \qquad (3.19)$$

At the peak of photon density, $\frac{dn_\emptyset}{dt} = 0$ and also $N^*(t) = N_{th}$. Thus equation (3.18) becomes,

$$n_\emptyset^{peak} = \frac{f_c}{\beta} [N_{th}(r - \ln r - 1) \qquad (3.20)$$

We can thus obtain Peak power by,

$$P_{peak} = \frac{n_\emptyset^{peak} V_c h^* \omega_l}{\tau_c} \qquad (3.21)$$

The Q-switched pulse duration (T) can easily then be obtained by dividing with pulse energy E obtained in equation (3.16).

3.2.2 Simulating Q-switching

Now that we have thoroughly analyzed the Q-switching rate equations we can easily simulate the Q-switching process.

The simplified algorithm is:

1) Define cavity parameters, time step duration dt, overpumping ratio.
2) Define variables $N^*[i]$ for threshold density and $n_\emptyset[i]$ for photon density.
3) Loop :
    a) Define dN^* on the basis of equation (3.6),

$$dN^* = \frac{-\beta n_\emptyset[i]N^*[i]}{\tau_c} - \frac{N^*[i]}{\tau_c} \quad (4.8)$$

    b) $N^*[i+1] = N^*[i] + dN^*$ (4.9)

    c) Define $dn_\emptyset$ on the basis of equation (3.2),

$$dn_\emptyset = \left(\frac{n_\emptyset[i]N^*[i]}{N_{th}\tau_c} - \frac{n_\emptyset[i]}{\tau_c}\right)dt \quad (5.0)$$

    d) $n_\emptyset[i+1] = dn_\emptyset + n_\emptyset$ (5.1)

End Loop {i=0 to max value needed}

3.2.3 Simulation results

Simulations were run to see if pulses with durations below 5nsecs could be obtained. The plots shown below shows the result of a specific cavity (parameters given below). The pulse building time was roughly about 30nsecs storing energy approximately equal to 18.72μJ. The pulse width was found out by calculating the FWHM of the photon density vs time steps plot and found out to be roughly about 4.57 nsecs.

Cavity length	1.8 cm
Gain length	1 cm
Mirror curvature	10 cm
Time step duration	0.5 nsecs
Cavity lifetime	1.49 nsecs
Output energy per pulse	18.72μJ
Pump power absorbed	24.12μJ
Beam waist	0.00075 cm
Pump pulse duration	4.57 nsecs
Q-switched pulse duration	20 nsecs

Table 1. Table containing data pertaining to the simulation run.

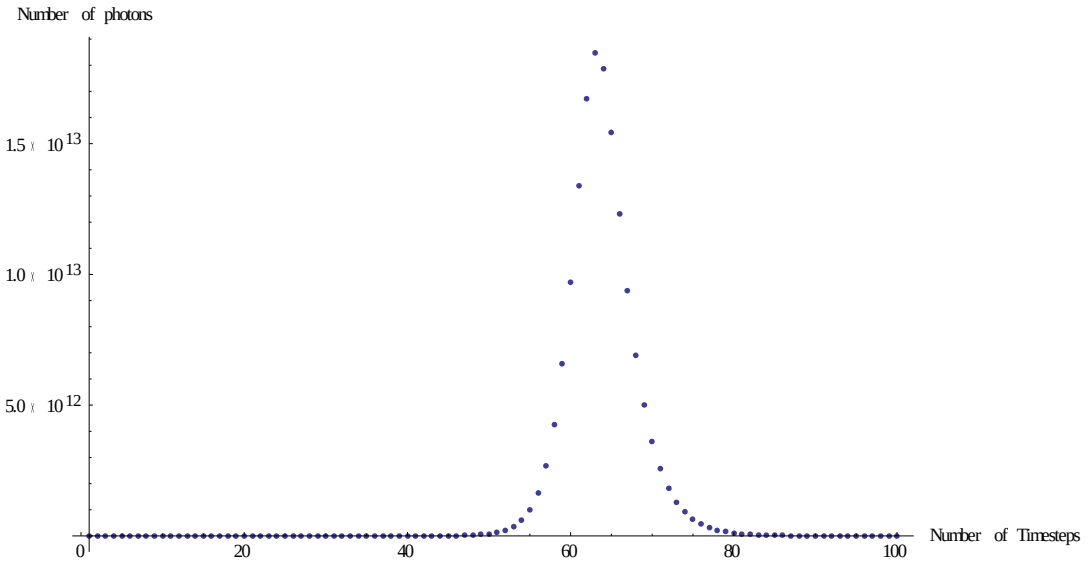

Fig.9: Plot of Number of photons vs Number of Timesteps.

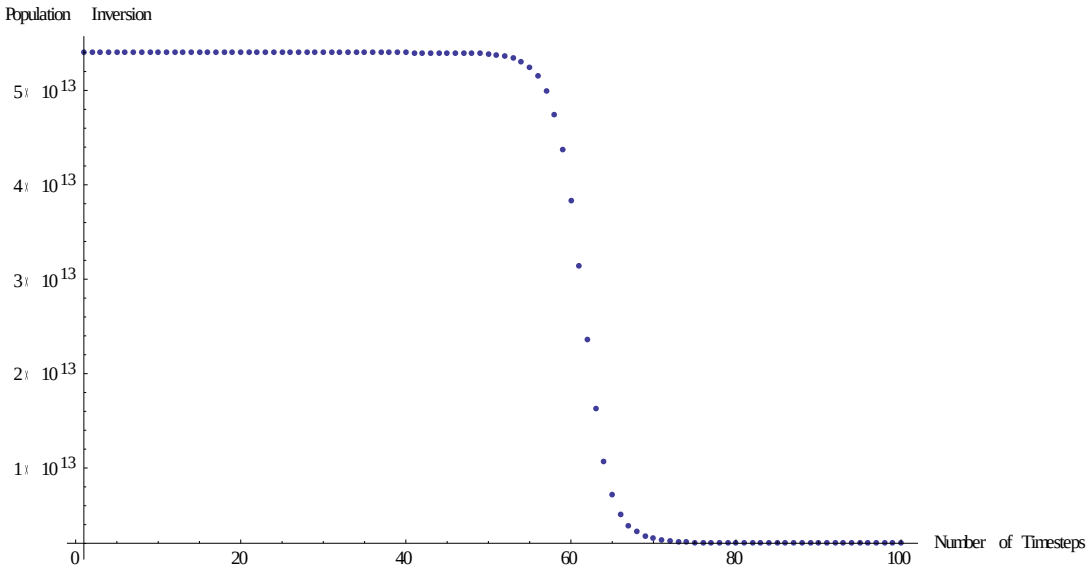

Fig.10: Plot of Population inversion vs Number of Timesteps.

Chapter 4

Experiment and Results

4.1 Absorption Spectroscopy

The absorption spectrum was obtained using a broad band source. The broad band source was modulated at 110 Hz using a chopper, the source beam was controlled using an aperture. The aperture controlled the beam to a circular shape, slightly smaller than the crystal. The light exiting from the crystal surface was then taken through a double convex lens setup and focused into 50 μm slit placed in front of the monochromater. Another 50 μm was placed at the monochromater exit, before the photo detector. The photo detector signal was fed into a lock in amplifier which was locked onto the chopping frequency.

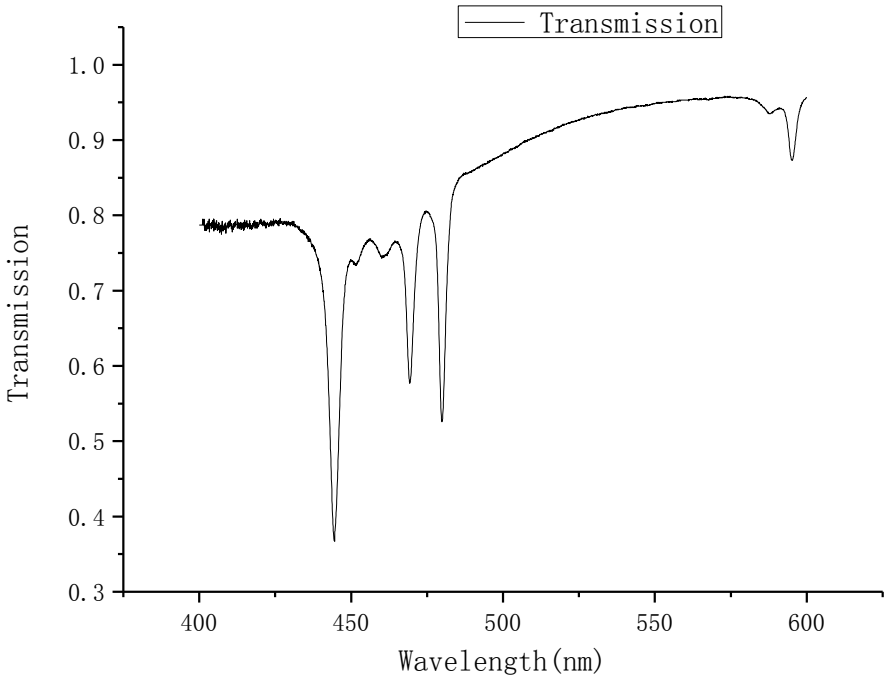

Fig.11: Transmission spectrum of Pr:YLF using unpolarized light source.

Since Pr:YLF is birefringent we also need to take care about the polarization of the light as the absorbance differs for π and σ polarization. Two polarizers were placed with their axis perpendicular to each other. Next the crystal was placed in between the polarizer. Since the crystal was randomly placed the output from the second polarizer should be non-zero. The crystal was then rotated till the output became zero, this denotes that the crystal axis was aligned with either the π or σ axis. Thus the absorption spectrum obtained would correspond to either one of them. Then, the second polarizer was removed and the absorption spectrum was obtained. The other polarization was then obtained by rotating the polarizer by 90 degrees.

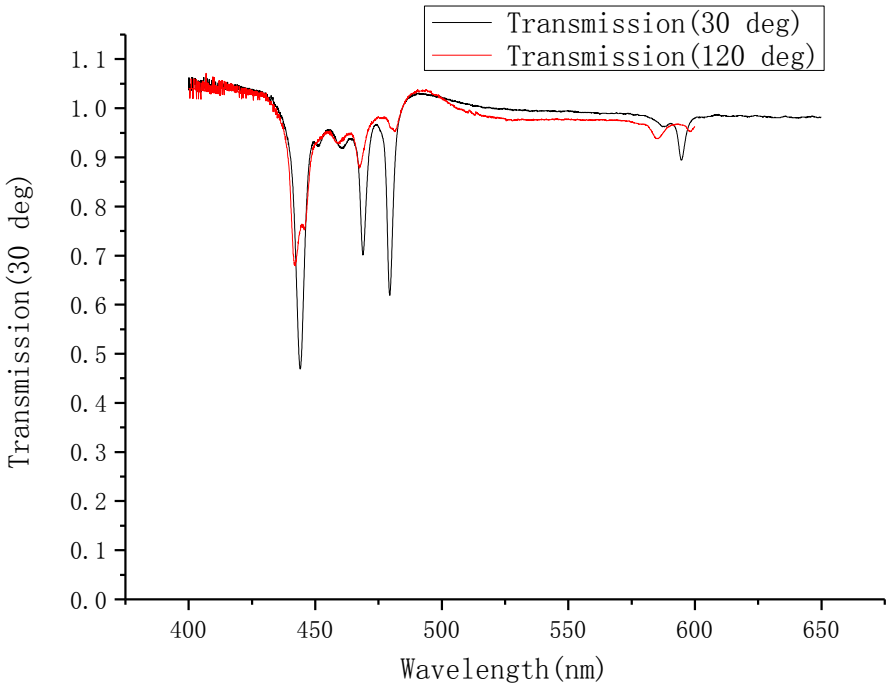

Fig.12: Transmission spectrum of Pr:YLF with polarizers at 30 and 120 degrees with respect to the fixed crystal axis.

We can see in the above figure how the absorption differs. We compared the obtained results with known literature sources and found out that the results match quite accurately. The table below lists the different absorption peaks and their absorption cross-sections for π polarization.

Wavelength (nm)	Absorption cross-section(in $10^{-19}cm^2$)
444	1.3
469	0.8
479	1.0
593	0.1

Table 2: List of absorption peaks and their cross-sections for π polarization

4.2 Emission spectroscopy

The fluorescence spectroscopy was obtained by pumping the crystal using the GaN laser pump, the luminescence from the crystal was collected into the monochromater and successively into the photo detector. The multiple energy transitions of praseodymium ion can be seen in the plot shown below. The polarized pump beam was oriented along the two crystal axes to gives us the π and σ polarization respectively. Again the results were consistent with reported literatures

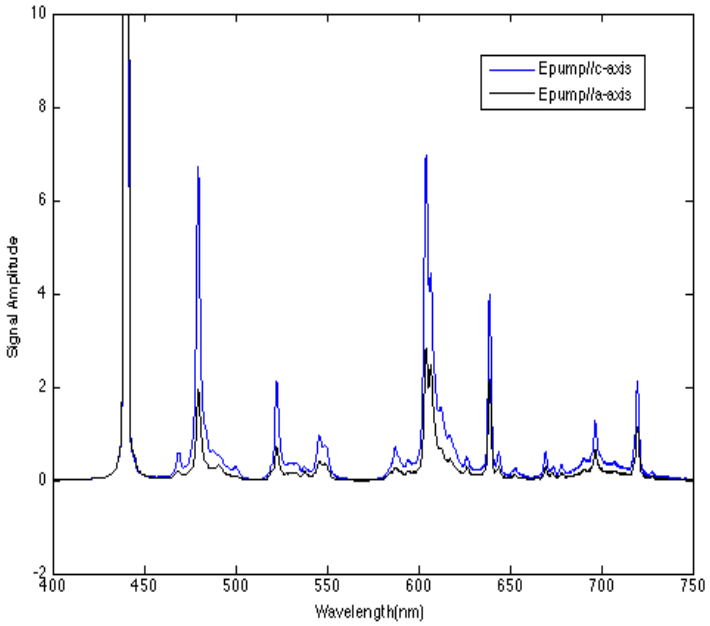

Fig.13: Pr:YLF emission spectrum

Despite our best efforts we were unable to completely prevent the pump beam from entering the monochromator. The large peak at 444nm is thus due to the pump beam. The emission peaks and their calculated cross-sections for π polarization.

Wavelength (nm)	Cross-section(in $10^{-19}cm^2$)
479	1.7
523	0.3
605	1.9
640	0.8
698	0.2
723	0.4

Table 3: List of emission peaks and their cross-sections for π polarization

4.3 Excited State Absorption

The ESA in Pr:YLF was measured using the pump probe technique which has already been discussed in section 2.4.2 . The figure below shows the setup used to carry out this experiment. The GaN blue diode laser was used as the pump to excite the ground state, the probe beam was modulated at 110 Hz while the pump beam was unmodulated. The crystal sample we used was a 1cm long, 0.2% doped Pr:YLF crystal from Photop Technologies.

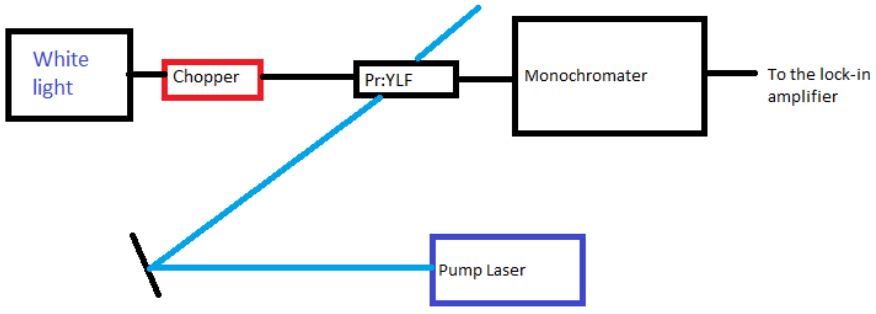

Fig.14: Simplified setup diagram

One of the major requirement for making accurate measurement is a good overlap between the region being pumped by the laser beam and the region being probed by the white light. It is for this reason we desire a uniformly shaped pump beam, we have already discussed the steps taken to achieve that in section 3.1, the other requirement is that the laser beam needs to be focused into the smallest possible spot size at the crystal. For a good overlap, we needed the laser beam to enter the polished crystal face at roughly the same spot as the probe beam. This was challenging since we could not afford to lose any power from the pump beam and also we needed to stop the pump beam from entering the monochromater. We calculated that a spot size of 100μm would produce sufficient population in the excited state. The pump beam was focused into the crystal using a combination of double convex lenses and silver coated curved mirrors.

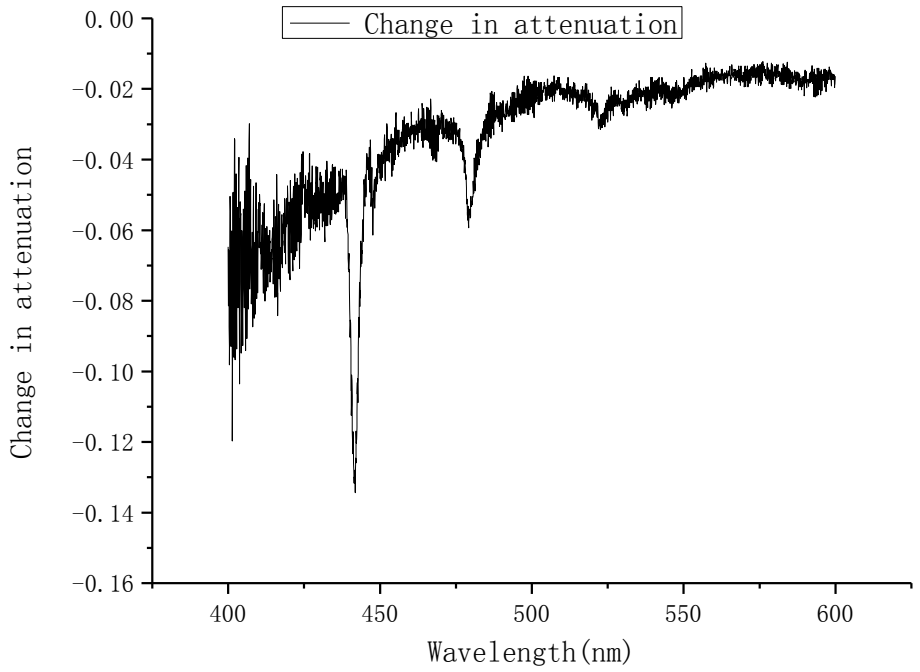

Fig.14: Change in Attenuation for π polarization

As discussed in section 2.4.2, we measured the change in absorbance using the pump-probe beam method. The figure above plots the change in attenuation vs wavelength for π polarization. As we already know a positive change in absorbance denotes the

presence of ESA, however no such readings were obtained. The experiment was repeated again for sigma polarization with the same result.

4.4 Conclusion

We characterized a 1cm long, 0.2 % doped Pr:YLF crystal for excited state absorbtion. We were unable to detect any presence of excited state absorption in the range of 400nm – 600 nm. We also obtained the absorption and fluorescence profile for the crystal. The obtained results were in agreement with previously published literatures [1, 2, 8, 9,10]. A number of simulations were run to determine the possibility of creating a short Q-switched pulse using this crystal, simulations show that pulses with durations as short as 4.57 nsecs can be made.

Bibliography

[1] J.L. Adam, W.L. Sibley, and D.R. Gabbe, J. Lumin. **33**,391 (1985)

[2] L. Esterowitz, R.Allen, M.Kruer, F. Bartoli, L.S. Goldberg, H.P. Jennsen, A. Linz and V.O. Nikolai, J Appl.Phys. **48**,650 (1977)

[3] R.I. Laming, S.B. Poole, and E.J. Tarbox, Optics Letters **1084**, Vol.13 (1988)

[4] J. Koetke, and G. Huber, Appl.Phys **61,**151 (1995)

[5] E. Georgiou, J.F. Pinto, and C.R. Pollock, Physics Review, **Vol.35** (1986)

[6] S. Nakamura, IEEE, **Vol.36**, No.3B (1997)

[7] S. Hooker and C. Webb, *Laser Physics*, second edition, 2010

[8] Hansen, Nils-Owe, Applied Optics, **49**, 20 (2010)

[9] A. Richter, E. Heumann, and G. Huber, Optics Express, **15**, 20 (2014)

[10] X.D. Li, X. Yu, R.P. Yan, R.W. Fan, and D.Y. Chen, Laser Phys. Lett. **8**, No.11 (2011)